Hetz C. 2012. Protein folding stress in neurodegenerative disease. IX Workshop on the Molecular Biology of Stress Responses. Porto Allegre, Brazil, May 27-30

Has the funding of this project led to the receipt of other funds? If so, what is the total amount?

No

Abstract (electronic and hard copy)

Defining the role of the endoplasmic reticulum (ER) stress and the UPR in Spinal Cord Injury

Claudio Hetz and Felipe A. Court, Institute of Biomedical Sciences, University of Chile and Department of Physiology, P. Universidad Católica de Chile, Santiago, Chile.

Summary. The mechanisms of injury-induced death of neurons within the spinal cord are poorly understood. Recent evidence from different laboratories implicates the participation of adaptive responses to stress at the endoplasmic reticulum (ER) in the disease process, a pathway known as the Unfolded Protein Response (UPR). In this project, we have defined the contribution of the UPR to cellular and functional dysfunction after Spinal Cord Injury (SCI) and analyzed the possible therapeutic effects of alleviating ER stress in mouse models of the pathology. Our results directly demonstrate for the first time that activation of the UPR operates as protective and very early tissue response against SCI, providing a novel target for therapeutic intervention. We demonstrated this hypothesis using biochemical analysis of ER stress signaling, the use of two independent genetic models to manipulate the UPR and the development of a novel prototypic gene therapy to attenuate ER stress locally in the affected spine tissue.

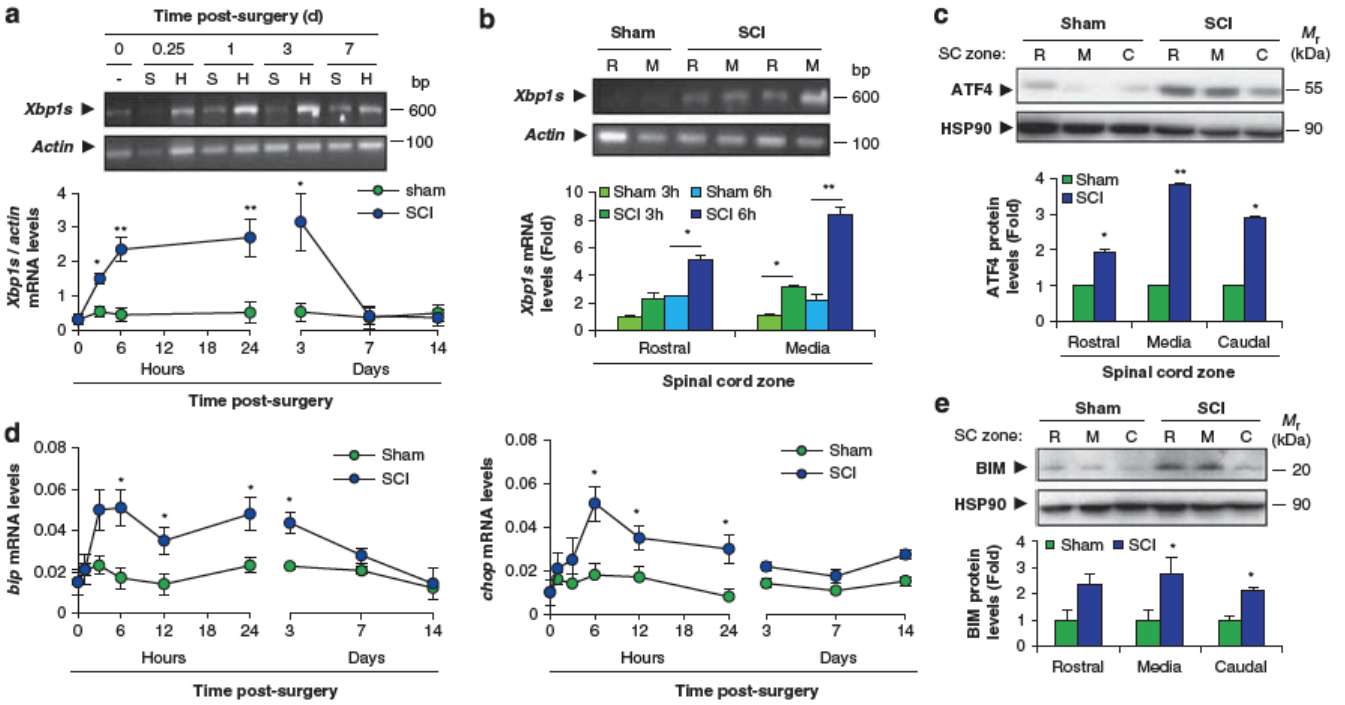

Figure 1 UPR activation after spinal cord hemisection. (a) Wild-type mice were spinal cord-hemisected (H) or sham-operated (S) at the T12 vertebral level. 0.25 (6 h), 1, 3, 7, and 14 days after the surgical procedure, tissue from the operated region of the spinal cord was extracted and processed to measure spliced *Xbp1* (*Xbp1s*) mRNA levels by RT-PCR. *Actin* mRNA was used for normalization. (b) The same procedure was used to study *Xbp1* mRNA splicing at 3 and 6 h after SCI at the injured region (media) and at a distance from the injury site (rostral) (lower panel). *Xbp1s* levels were quantified and normalized using *actin* mRNA levels. (c) ATF4 protein levels were measured by western blot and semiquantified by normalizing with HSP90 protein levels. Blot and graph at 6 h after sham or hemisection from rostral (R), operated (M) and caudal (C) regions are shown. (d) *bip* and *chop* mRNA levels were quantified at the indicated times after damage by real-time PCR. (e) BIM protein levels at 6 h after SCI were measured by western blot. Protein levels were normalized with HSP90 levels and then normalized to the sham-operated condition. Mean ± S.E.M. $^{*}P<0.05$; $^{**}P<0.005$; Student's *t*-test; $n=3$ animals per group for protein and mRNA analysis

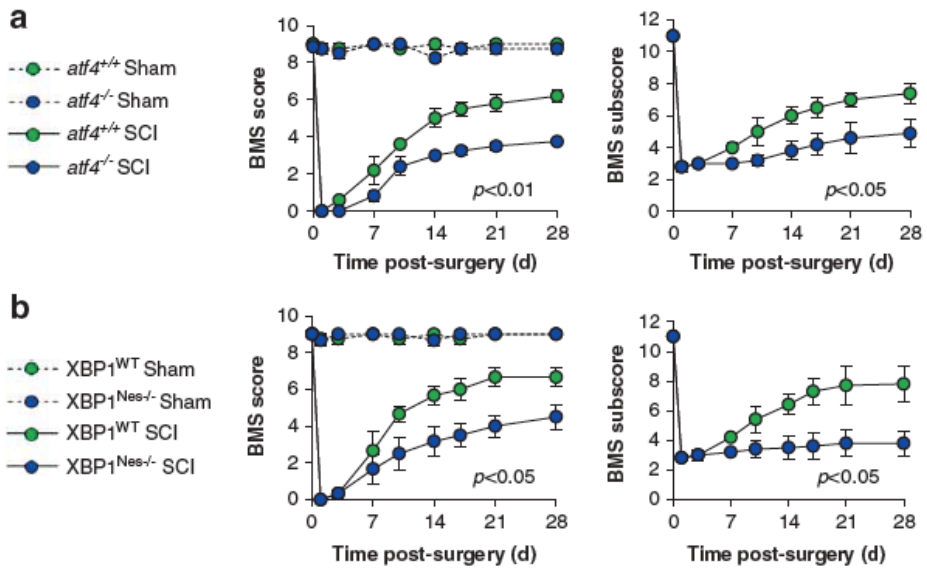

Figure 2 Role for UPR in locomotor recovery after SCI. (**a**) *atf4*$^{+/+}$ and *atf4*$^{-/-}$ mice were hemisected at the T12 vertebral level. Their locomotion recovery pattern was monitored before (0 day) and after spinal cord hemisection using the BMS open-field test to determine their locomotor capabilities (left plot). The BMS subscore was quantified to assess locomotor recovery of finer movements (right plot). (**b**) The same as in (**a**), but comparing XBP1^{WT} with XBP1$^{Nes-/-}$ mice. Mean ± S.E.M. Statistical differences were analyzed by a two-way repeated-measures ANOVA followed by Bonferroni's *post hoc* test; *P*-values for SCI group comparison are indicated in the graph; $n = 8$ animals per group

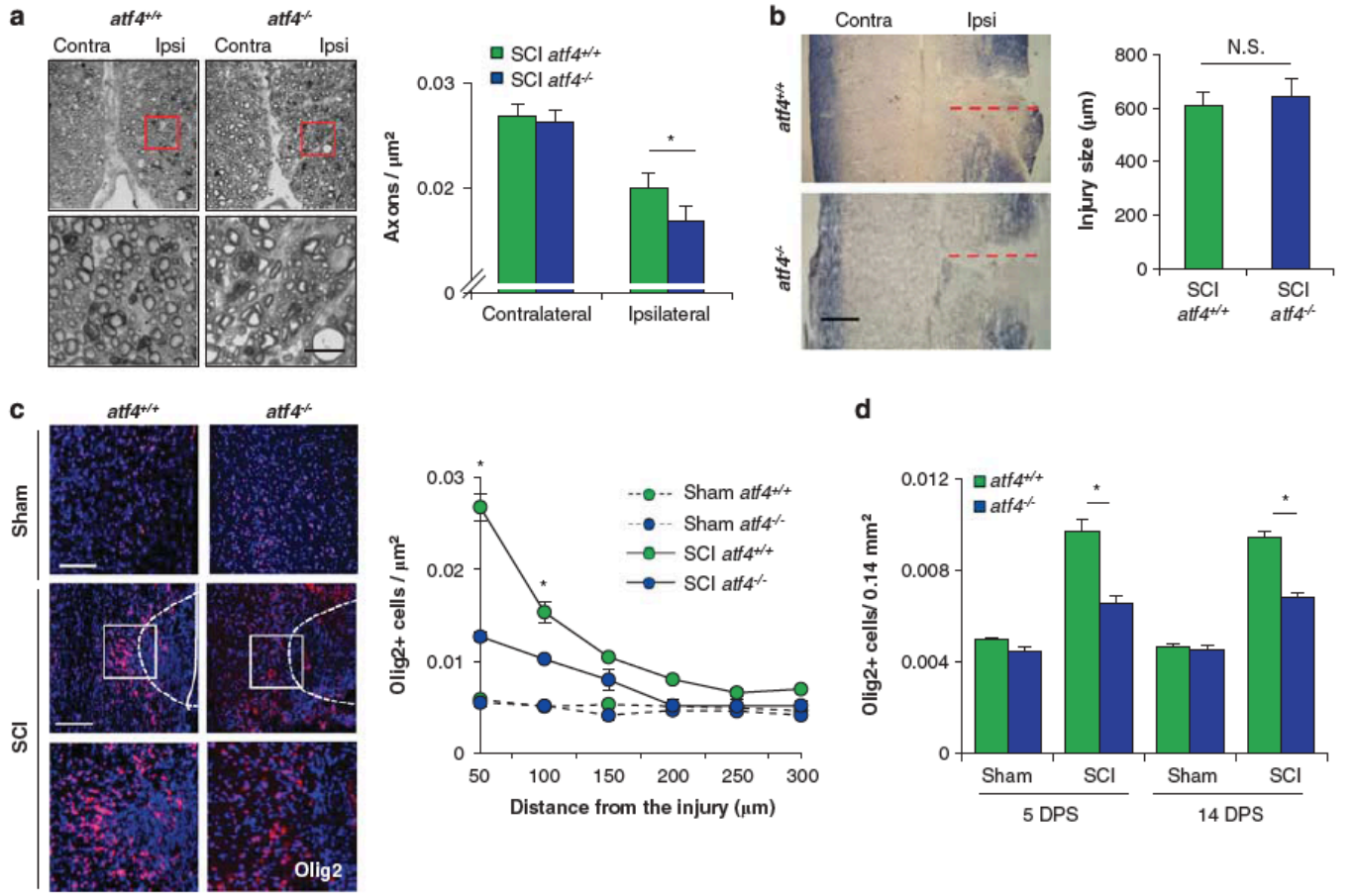

Figure 3 Altered cellular environment in ATF4-deficient mice after SCI. (**a**) *atf4*$^{+/+}$ and *atf4*$^{-/-}$ mice were spinal cord-hemisected or sham-operated at the T12 vertebral level. At 14 days after surgery, spinal cord tissue was stained with toluidine blue to study axonal integrity (left panel). Intact axons from corticospinal tracts were quantified and expressed as axonal density values (right panel). (**b**) Spinal cord tissue from hemisected *atf4*$^{+/+}$ and *atf4*$^{-/-}$ mice were longitudinally sectioned to analyze the injury size by eriochrome/cyanine myelin staining. Transversal injury length was measured from the edge of the spinal cord to the midline as shown by the red-dotted line. (**c**) *atf4*$^{+/+}$ and *atf4*$^{-/-}$ mice were spinal cord-hemisected or sham-operated at the T12 vertebral level. At 5 days after surgery, spinal cord tissue processed for immunofluorescence for Olig2, to study oligodendrocytes and its progenitors (red); nuclei were counterstained using Hoechst (blue). Olig2-positive particles co-localizing with Hoechst were quantified every 50 μm starting at the injury site. (**d**) The same procedure as (**c**), but total Olig2/Hoechst-positive particles were quantified in a semicircular area of 300 μm radius surrounding the injury zone at 5 and 14 days post-surgery (DPS). Mean ± S.E.M. *$P<0.05$; Student's *t*-test; $n=3$ animals per group. Scale bars, 20 μm in (**a**), 200 μm in (**b**), and 100 μm in (**c**). Bars indicate S.E.M.

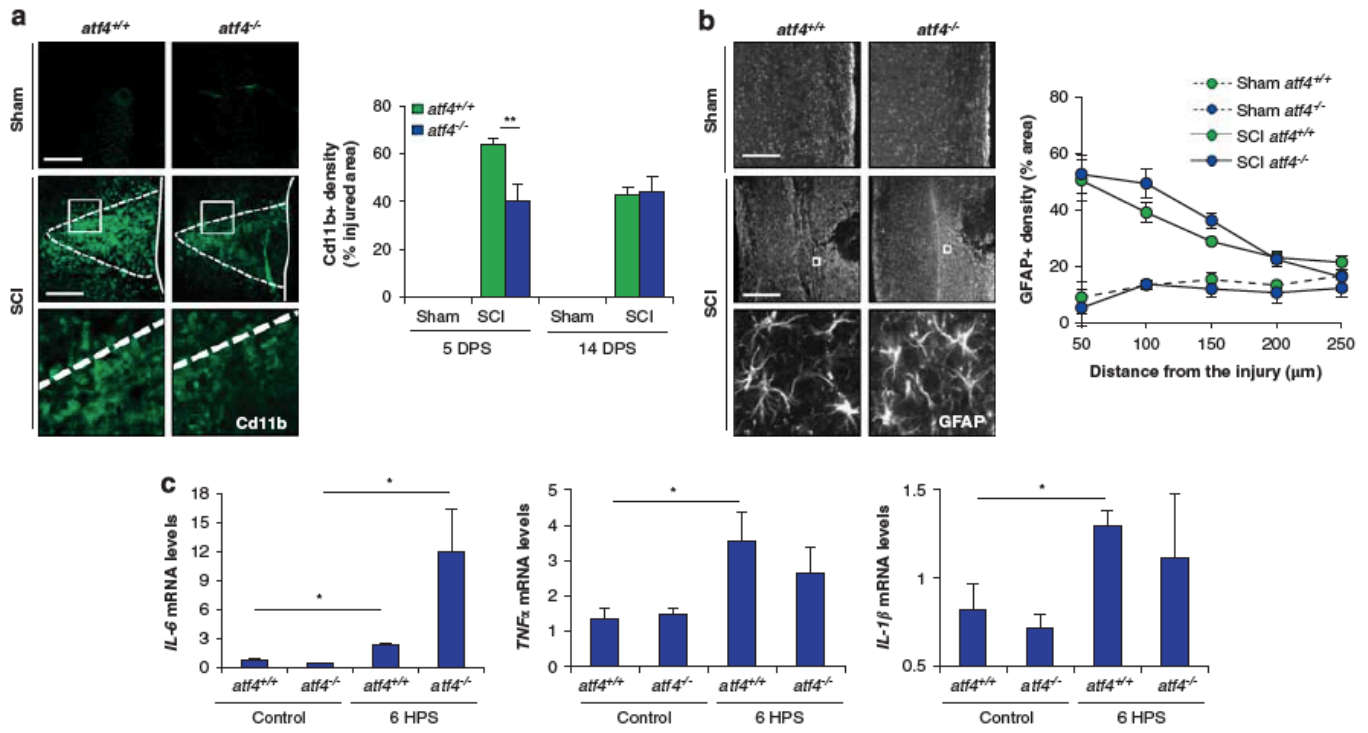

Figure 4 Altered inflammatory response in UPR-deficient mice after SCI. (**a**) $atf4^{+/+}$ and $atf4^{-/-}$ mice were spinal cord-hemisected or sham-operated at the T12 vertebral level. At 5 days after surgery, spinal cord tissue was extracted and processed for immunofluorescence for the microglial marker Cd11b at the injury zone (left panel). The density for Cd11b staining was quantified at the injured zone delimited with a dotted line (right plot) at 5 and 14 days post-surgery (PDS). (**b**) Activated astrocytes were studied by GFAP immunostaining. GFAP-positive label surrounding the injury zone was quantified every 50 μm from the injury (right panel). (**c**) Inflammatory cytokines were analyzed from injured spinal cord tissue of $atf4^{+/+}$ and $atf4^{-/-}$ mice by real-time PCR 6 h after surgery (HPS). Mean ± S.E.M. $^{*}P<0.05$; $^{**}P<0.005$; Student's *t*-test; $n=3$ animals per group. Scale bars, 300 μm in (**a**) and 20 μm in (**b**)

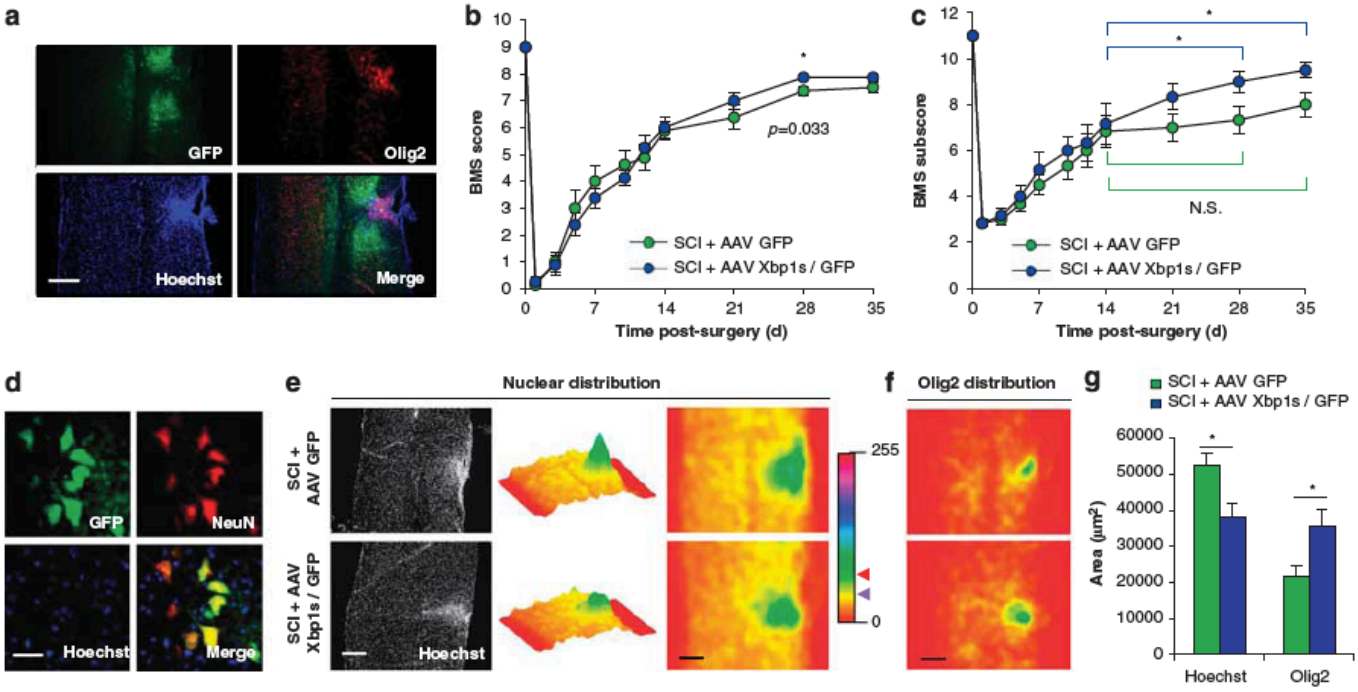

Figure 5 *Xbp1s* gene transfer with AAVs enhances locomotion recovery after SCI. Wild-type mice were hemisected at the T12 vertebral level and immediately injected into the injury site with 2 μl (10^{12} DRP/ml) of AAV-GFP or AAV-Xbp1s/GFP. (**a**) Transduction levels were analyzed 35 days after injection by GFP expression (green), immunolabelled with an Olig2 antibody (red) and counterstained with Hoechst (blue) in the AAV-Xbp1s/GFP injections. (**b**) Locomotion recovery pattern was monitored before (0 day), and after spinal cord hemisection and viral transduction with AAV-GFP or AAV Xbp1s/GFP, using the BMS open-field test. (**c**) In the same groups, the BMS subscore was quantified to assess locomotor recovery of finer movements. (**d**) Neuronal-specific GFP transduction was confirmed by NeuN immunostaining (red) of spinal cord tissue injected with AAV Xbp1s/GFP (in green); nuclei were counterstained using Hoechst (blue). (**e**) Nuclear density in the injured region was analyzed by averaging Hoechst-positive nuclei intensity from eight mice for each condition and displayed as a surface plot. The *Z* axis represents average intensity in a pseudo-colored map. (**f**) Using the same approach as in (**e**), Olig2-positive cell density was studied in AAV-GFP or AAV Xbp1s/GFP-injected mice. (**g**) To quantitatively compare cellular density profiles, intensity plots of Hoechst- or Olig2-stained spinal cords from (**e**) and (**f**) were threshold at a fixed level (red arrowhead for Hoechst and purple arrowhead for Olig2 in the color map shown in (**e**)), and the resulting positive area was measured and plotted. Mean ± S.E.M. $^*P < 0.05$. Two-way repeated-measures ANOVA followed by Bonferroni's *post hoc* test for panels (**b**) and (**c**); $n = 8$ animals per group. Student's *t*-test for panel (**g**); $n = 8$ animals per group. Scale bars, 300 μm in (**a**), 20 μm in (**d**), and 300 μm in (**e**) and (**f**)

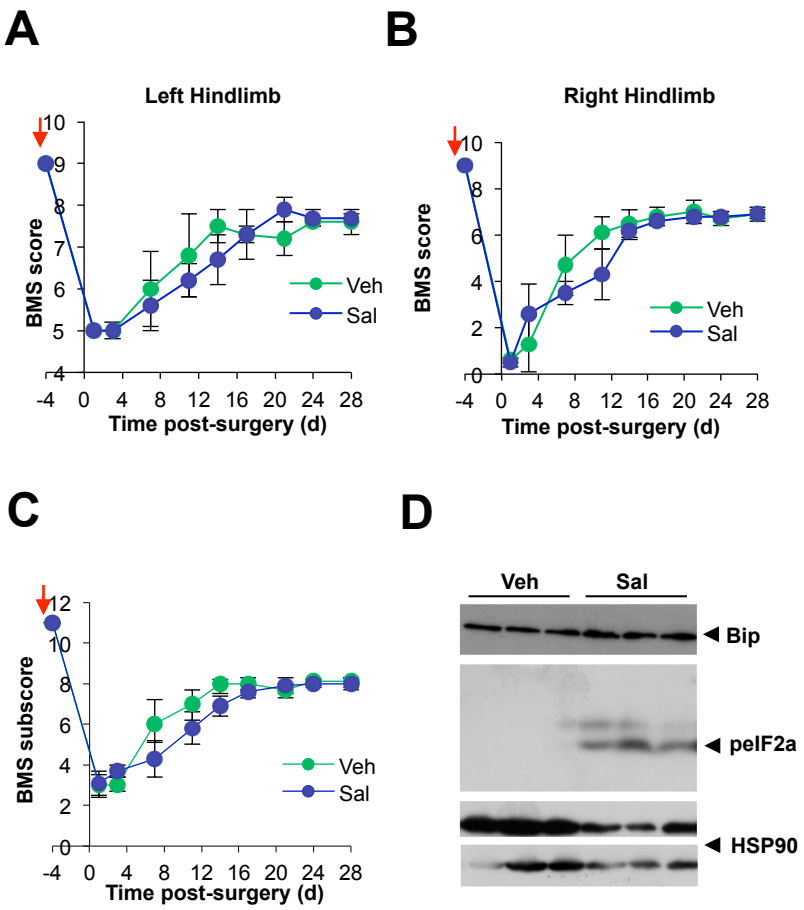

Figure 6. No effect of salubrinal in SCI. (A) And (B) Mice were daily i.p. injected with 2 mg/Kg Salubrinal (red arrow). At day 4, mice were hemisected at the T12 vertebral level. Their locomotion recovery pattern was monitored before and after spinal cord hemisection using the Basso Mouse Scale (BMS) open field test to determine their locomotor capabilities in left and right hindlimb. (C) The BMS subscore was quantified to assess locomotor recovery of finer movements (D) After 28 days, mice were euthanized to evaluate spinal cord protein levels by Western blot. n=7 per group in the liver.

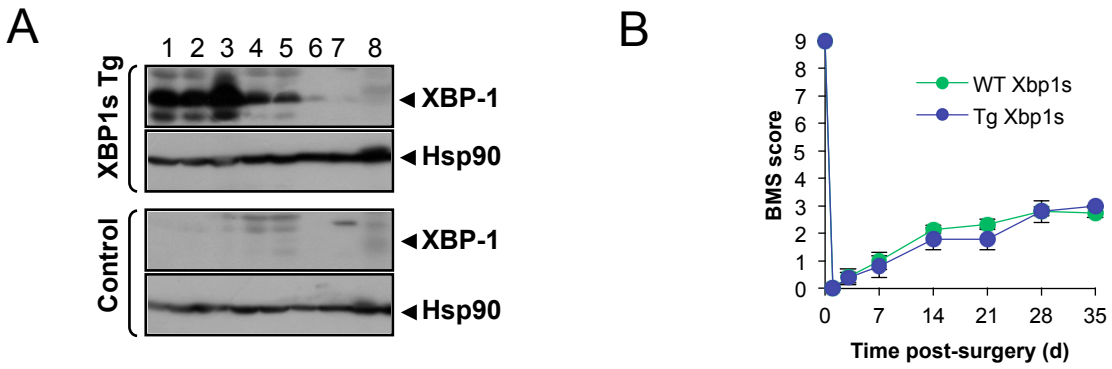

Figure 7. Assessment of the suceptibility of a new XBP1s transgenic mice to SCI. (A) Different tissues from a brain specific XBP1s transgenic mice or a litter mate WT control were analyzed by Western blot to monitor the tissue distribution of XBP1s expression. Hsp90 was used as loading control. Lines: 1: Cortex, 2 Hippocampus, 3 Cerebellum, 4 Brain stem, 5 Spinal cord, 6 Heart, 7 Lung, and 8 Liver.
(B) WT and Tg Xbp1s mice were hemisected at the T12 vertebral level. Their locomotion recovery pattern was monitored before and after spinal cord hemisection using the Basso Mouse Scale (BMS) open field test to determine their locomotor capabilities. n=7 in WT and n=5 in Xbp1s Tg mice.

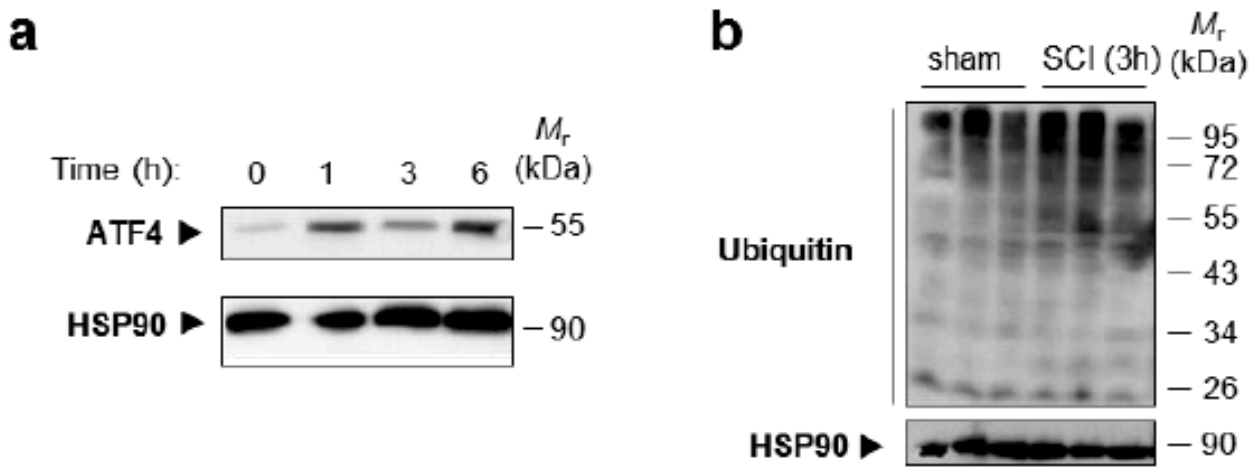

Figure S1 ATF4 expression and accumulation of ubiquitinated proteins in the spinal cord after hemisection. (**a**) Wild type mice were spinal cord hemisected at the T12 vertebral level. 1, 3 and 6 hours after surgery, spinal cord tissue from the operated region was extracted and processed. ATF4 protein levels were analyzed by Western blot and semi-quantified by normalizing to HSP90 protein levels. Blot at 1, 3 and 6 hours after spinal cord hemisection from the operated zone is shown. (**b**) Protein ubiquitination was studied by Western blot in tissue samples from spinal cord hemisected or sham operated wild type mice at the T12 vertebral level.

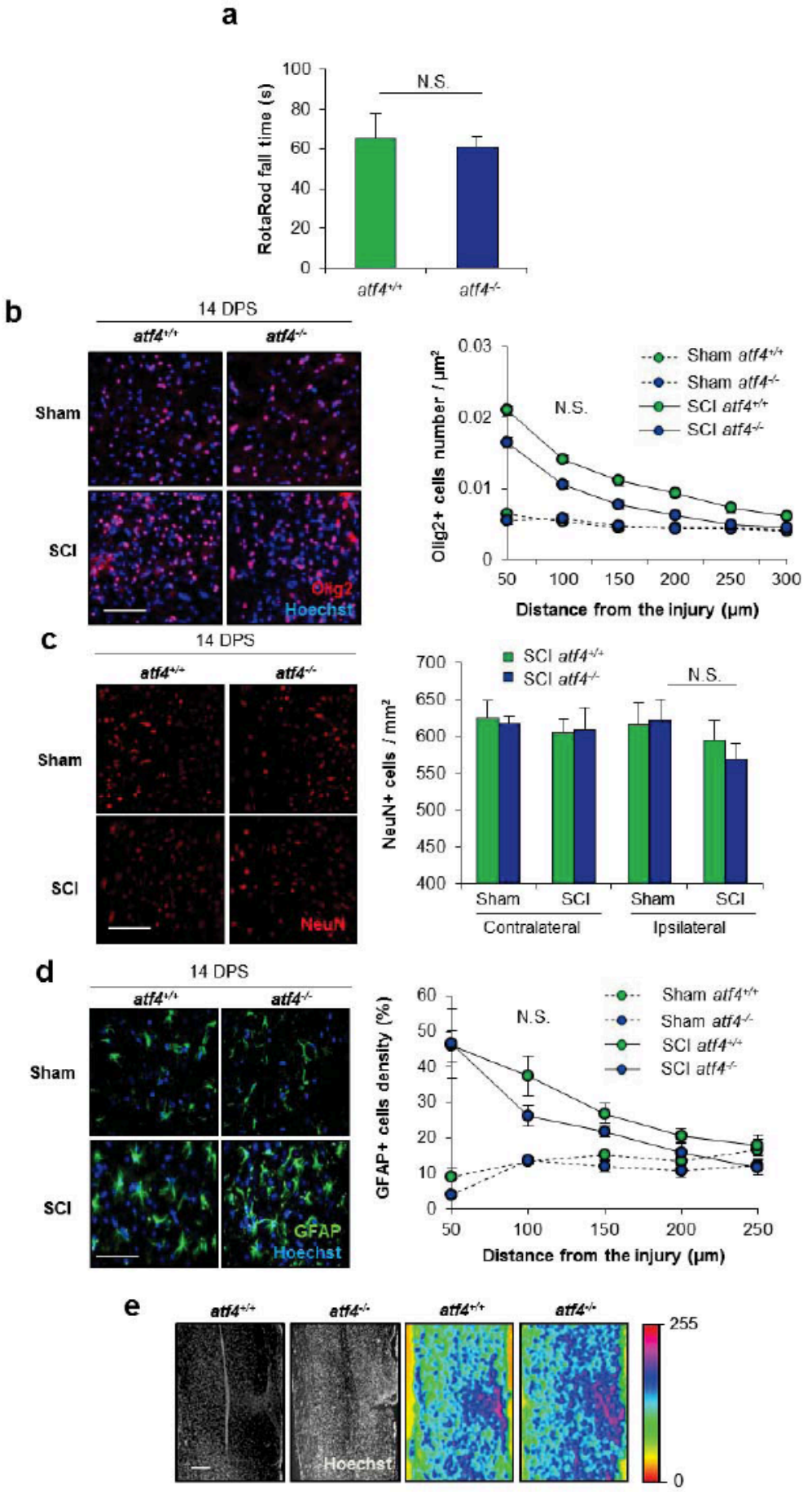
a
RotaRod fall time (s)
N.S.
atf4+/+
atf4-/-
b
14 DPS
Sham
SCI
Olig2
Hoechst
Olig2+ cells number / µm²
Sham atf4+/+
Sham atf4-/-
SCI atf4+/+
SCI atf4-/-
Distance from the injury (µm)
c
NeuN
NeuN+ cells / mm²
Contralateral
Ipsilateral
d
GFAP
GFAP+ cells density (%)
e
Hoechst
255
0

Figure S2 Altered cellular environment at 14 days post-SCI in UPR deficient mice. (**a**) Non-injured *atf4*$^{+/+}$ and *atf4*$^{-/-}$ mice were trained and scored by the RotaRod test (ramp mode). (**b**) *atf4*$^{+/+}$ and *atf4*$^{-/-}$ mice were spinal cord hemisected or sham operated at the T12 vertebral level. 14 days after surgery, spinal cord tissue processed for immunofluorescence, to study oligodendrocytes (OL) and OL progenitors (red); nuclei were counterstained using Hoechst (blue). Olig2-positive particles colocalizing with Hoechst were quantified every 50 µm starting at the injury site. (**c**) Spinal cord neurons were analyzed by immunofluorescence using an antibody against NeuN. Neuronal density was analyzed in *atf4*$^{+/+}$ and *atf4*$^{-/-}$ mice 14 days after SCI in both contralateral and ipsilateral sides. (**c**) *atf4*$^{+/+}$ and *atf4*$^{-/-}$ mice were spinal cord hemisected or sham operated at the T12 vertebral level. 14 days after surgery, spinal cord tissue processed for immunofluorescence using an antibody against GFAP to study astrocytes (green); nuclei were counterstained using Hoechst (blue). GFAP-positive cells were quantified every 50 µm starting at the injury site (right panel). (**d**) Nuclear density in the injured region was analyzed by averaging Hoechst-positive nuclei intensity from 3 mice for each condition and displayed as a surface plot. The Z-axis represents average intensity in a pseudo-colored map. Mean +/- SEM. *, $p<0.05$; **, $p<0.005$; Student's *t*-test; n=3 animals per group for immunofluorescence analysis; n=10 for RotaRod test. Scale bars, 100 µm in (**a**), 200 µm in (**b**), 20 µm in (**c**), 300 µm in (**d**).

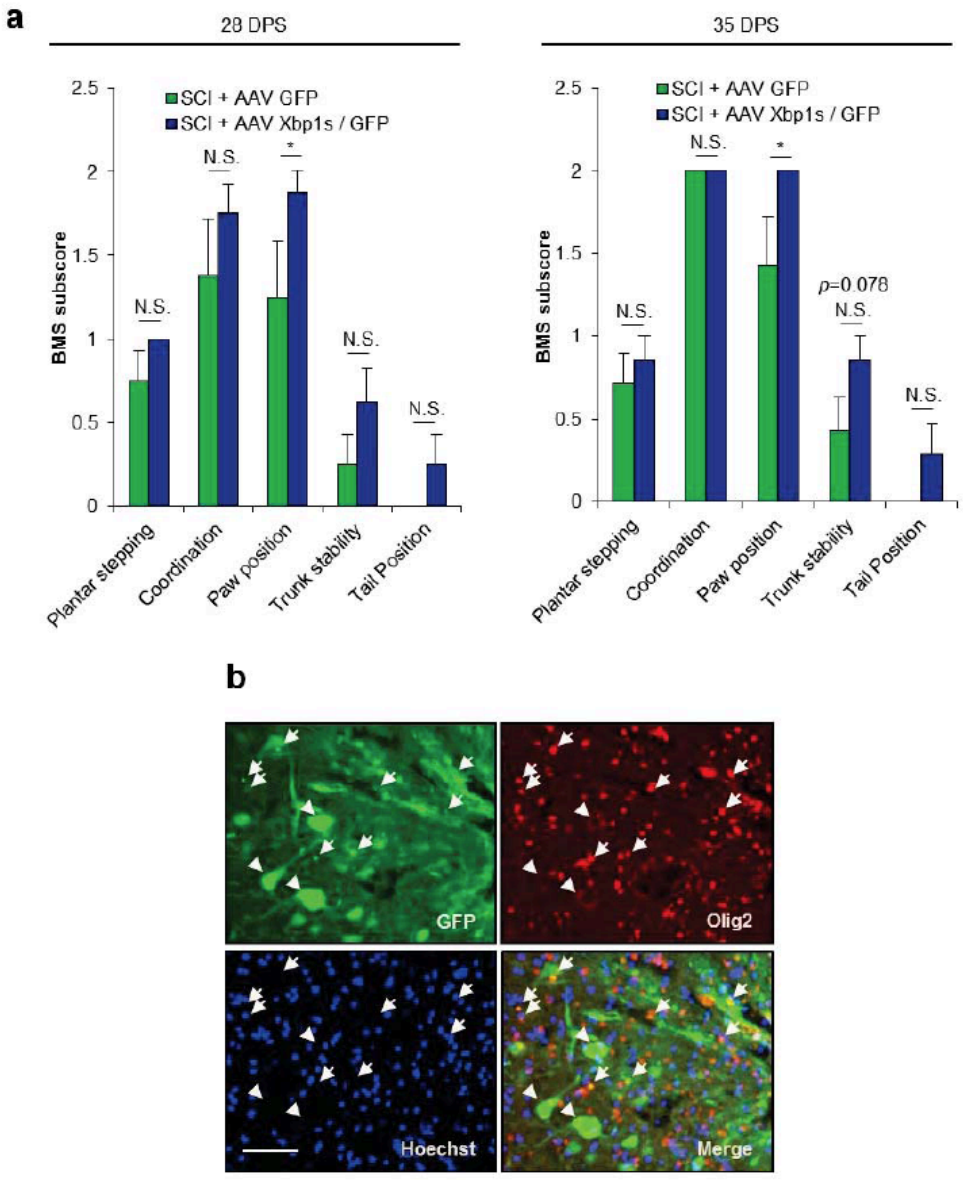

Figure S3 *Xbp1s* gene transfer with AAVs enhances locomotion recovery after SCI. (**a**) Wild type mice were hemisected at the T12 vertebral level and immediately injected into the injury site with 2 µl (10^{12} DRP/mL) of AAV-GFP or AAV-Xbp1s/GFP. Locomotion recovery pattern was monitored before (0d) and after spinal cord hemisection and viral transduction with AAV-GFP or AAV Xbp1s/GFP using the Basso Mouse Scale (BMS) open field test. The BMS subscore, which assess fine locomotor capabilities was scored and individual parameters of this subscore are presented at 28 and 35 days post-SCI. Mean +/- SEM. *, $p<0.05$; **, $p<0.005$. n=8 animals per group. Student's *t*-test. (**b**) Transduction levels were analyzed 35 days post-injection by GFP expression (green), immunolabelled with an Olig2 antibody (red) and counterstained with Hoechst (blue) in the AAV-Xbp1s/GFP injections. Higher exposure of GFP fluorescence reveal AAV transduction of Olid2-positive cells (arrows) in addition to neurons (arrowheads). Scale bar, 50 µm.

a

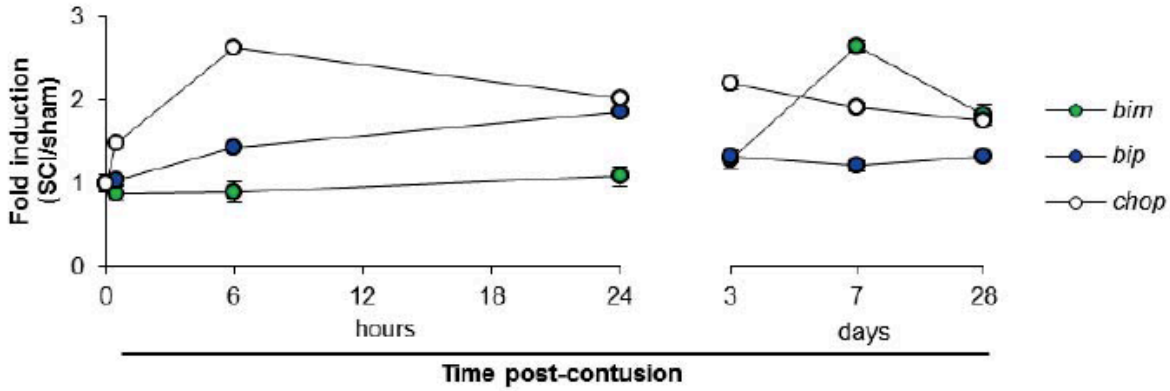

b

Fold induction (SCI / sham)	Time post-surgery: hours 0	0.5	6	24	days 3	7	28
edem	1	0.84	0.88	1.22	1.87	1.62	1.32
sec61	1	0.92	0.99	2.14	1.57	2.13	1.53
grp58	1	0.78	0.92	1.23	2.10	2.81	1.29
xbp-1	1	1.05	1.13	1.50	1.16	1.04	1.34
grp78	1	1.06	1.47	1.90	1.36	1.24	1.36
ho1	1	1.08	2.38	5.68	3.23	1.93	1.39
bim	1	0.89	0.9	1.11	1.29	2.65	1.83
atf4	1	1.16	1.74	2.06	1.24	1.20	0.89
chop	1	1.49	2.64	2.03	2.21	1.95	1.75
calnexin	1	1.03	1.11	1.26	0.86	0.95	1.01
calreticulin	1	1.13	1.09	1.57	1.06	1.18	1.29
actin	1	0.97	0.96	1.16	0.93	0.85	1.18

Figure S4 Analysis of UPR markers from the microarray GDS2159 in the T8 spinal cord segment up to 28 days after moderate contusion injury. (**a**) Expression levels of the indicated genes at different times after moderate spinal cord contusion in wild type mice obtained from the GDS2159 microarray data. Relative expression levels were normalized with actin mRNA levels and then sham normalized. (**b**) Table showing relative fold-induction values of UPR markers after moderate spinal cord contusion in wild type mice relative to control values (non-injured). Data was obtained from the microarray GDS2159 available at GEO dataset browser (http://www.ncbi.nlm.nih.gov/sites/GDSbrowser?acc=GDS2159).